Applied Mathematical Sciences, Vol. 4, 2010, no. 18, 879 - 893

Navier-Stokes Characteristic Boundary Conditions for Simulations of Some Typical Flows

Chen Lin and Tang Dengbin

Nanjing University of Aeronautics and Astronautics
Nanjing 210016, P. R. China
chenlincfd@gmail.com

Abstract

The improved Navier-Stokes characteristic boundary conditions (NSCBC) method for direct numerical simulation of viscous flows, combining six order non-dissipative compact schemes with eight order filters ,are studied in this paper. The new boundary conditions including transverse and viscous effects are applied to a comprehensive set of test problems, such as vortex-convection, counter flow, pressure wave propagation and boundary layer flow. The computational results show that these boundary conditions, which relate to the resolution, stability and reflection of numerical simulation, have wider applicability and higher numerical precision.

Keywords: Navier-Stokes characteristic boundary conditions (NSCBC); non-dissipative compact schemes; direct numerical simulation; viscous flow

1. INTRODUCTION

The treatment of boundary conditions is one of the most recurrent issues in computational fluid dynamics. Computational accuracy, in general, is strongly sensitive to boundary solution, which may be spoiled by spurious numerical reflections. These spurious reflections of physical information, adversely affect the accuracy and stability of the solutions. This matter is of vital to using high order non-dissipation schemes in direct numerical simulation of Navier-Stokes equations, because non-dissipation schemes have very low numerical dissipation,

it need more accurate boundary conditions to ensure numerical stability[1]. This motivates the necessity for strategies to reduce reflection and set up transparent boundary conditions.

Several approaches were proposed to tackle boundary conditions. Techniques based on characteristics waves motivated much attention. Previous studies on the characteristic boundary conditions focused on how to suppress acoustic wave reflections at open boundaries. Initially for hyperbolic systems of Euler equations, these approaches decompose the flow in terms of characteristic waves traveling in the direction normal to the boundary, and reduce the boundary problem to a suitable dealing with the incoming waves. The identification of incoming waves allows, in principle, a direct control over boundary reflection, as the boundary condition can be designed to prevent incoming perturbations or to damp smoothly their amplitude. This one-dimensional approximation of the characteristic boundary conditions was successfully applied in multi-dimensional Euler equations by Thompson [2, 3].

An extension to the Navier–Stokes equations was discussed by Poinsot and Lele[1], who developed a systematic approach to account for viscous terms under the locally one-dimensional inviscid (LODI) assumptions, known as Navier–Stokes characteristic boundary conditions. The mathematical well-posedness of boundary conditions in fluid dynamics was studied by J.Oliger et al [4] and L.Halpern[5]. The stability of the viscous boundary conditions was investigated by P.Dutt[6]. The NSCBC approach was further extended to consider multi-component reacting flows [7-8], and subsonic nonreflecting inflow conditions were also derived as a variation within the generalized formulation [9].

As an example of refinement of the NSCBC approach, Sutherland and Kennedy [10] recognized that the chemical source terms must be considered in the LODI formulation in order to reproduce realistic flame propagation through the boundary. Yoo et al [11] studied the counterflow diffusion flame simulations. It was found that transverse convection terms must also be properly accounted for in the modified LODI expression to achieve correct solution behavior. It was also observed that, similar to the pressure relaxation used in the existing nonreflecting boundary conditions, a proper relaxation treatment for the transverse terms was also necessary in order to ensure solution stability. These results suggest that, for a successful application to general turbulent combustion problems, the entire formulation of the characteristic boundary conditions may have to be re-examined for a complete resolution of these issues. Yoo and Im[12] attempted to revisit the full NSCBC formulation in a generalized context, by reconsidering many terms that have been neglected before. Generalized LODI approximations that were applicable for a wide range of reacting flow conditions were derived.

In this paper, the improved NSCBC method which is compatible with high order non-dissipative compact schemes [13] is addressed. A couple of typical

flows are tested to certificate the feasibility of the algorithm. It is concluded from computational results that this method has high resolution and more convenient applicability.

2. CHARACTERISTIC BOUNDARY CONDITIONS

The compressible Navier-Stokes equations can be transformed into a characteristic form, written as (in x-direction) [10]:

$$\frac{\partial}{\partial t}\begin{bmatrix} u \\ v \\ w \\ \rho \\ p \end{bmatrix} + \begin{bmatrix} (L_5^{(x)} - L_1^{(x)})/\rho c \\ L_3^{(x)} \\ L_4^{(x)} \\ L_2^{(x)} + (L_5^{(x)} + L_1^{(x)})/c^2 \\ L_5^{(x)} + L_1^{(x)} \end{bmatrix} + \begin{bmatrix} \mathbf{V}_t \cdot \nabla_t u \\ \mathbf{V}_t \cdot \nabla_t v + (1/\rho)\partial p/\partial y \\ \mathbf{V}_t \cdot \nabla_t w + (1/\rho)\partial p/\partial z \\ \nabla_t \cdot (\rho \mathbf{V}_t) \\ \mathbf{V}_t \cdot \nabla_t p + \gamma p \nabla_t \cdot \mathbf{V}_t \end{bmatrix} = \begin{bmatrix} d_u \\ d_v \\ d_w \\ d_\rho \\ d_p \end{bmatrix} \tag{1}$$

where (x, y, z) are the spatial coordinates in a rectangular Cartesian system, t is time, ρ is the mass density, (u,v,w) are the components of flow velocity, p is the pressure, $\mathbf{V}$ is the velocity vector, $c = (\gamma RT)^{1/2}$ is the speed of sound and the subscript t is represents tangential (y- and z-) directions. This formula can also be used for reaction flow if reaction source terms are added.

The viscous terms is equation (1) are given by

$$\begin{bmatrix} d_u \\ d_v \\ d_w \\ d_\rho \\ d_p \end{bmatrix} = \begin{bmatrix} (1/\rho)\nabla_j \cdot \tau_{jx} \\ (1/\rho)\nabla_j \cdot \tau_{jy} \\ (1/\rho)\nabla_j \cdot \tau_{jz} \\ 0 \\ (\gamma - 1)[\tau_{jk} : \nabla_j u_k - \nabla_j \cdot q_j] \end{bmatrix} \tag{2}$$

where τ_{jk} is the shear stress , ∇_j is the Laplace operator, q_j is the heat flux, j,k=1,2,3.

The $L_k^{(x)}$ in equation (1) are the wave-based quantities obtained from a characteristic analysis of the x-direction governing equations. These quantities give the temporal rate of the amplitudes of the different acoustic, convective or entropy waves at the outcome boundary, and are defined as follows:

$$\begin{aligned} L^{(x)} &= (L_1^{(x)}, L_2^{(x)}, L_3^{(x)}, L_4^{(x)}, L_5^{(x)})^T \\ &= [\lambda_1^{(x)} \cdot \frac{1}{2}(\frac{\partial p}{\partial x} - \rho c \frac{\partial u}{\partial x}), \lambda_2^{(x)}(\frac{\partial \rho}{\partial x} - \frac{1}{c^2}\frac{\partial p}{\partial x}), \lambda_3^{(x)}\frac{\partial v}{\partial x}, \lambda_4^{(x)}\frac{\partial w}{\partial x}, \lambda_5^{(x)} \cdot \frac{1}{2}(\frac{\partial p}{\partial x} + \rho c \frac{\partial u}{\partial x})]^T \end{aligned} \tag{3}$$

where $\lambda_k^{(x)}$ are the characteristic velocities:

$$\lambda_1^{(x)} = u - c, \quad \lambda_2^{(x)} = \lambda_3^{(x)} = \lambda_4^{(x)} = u, \quad \lambda_5^{(x)} = u + c \tag{4}$$

Therefore, the problem of specifying inflow/outflow conditions is now reduced to the problem of determining the wave amplitude variations. According to characteristic system, the identification of the wave amplitude $L_i^{(x)}$ depends on the sign of $\lambda_i^{(x)}$. For the outward wave, $L_i^{(x)}$ is calculated by using one-side difference method from inside the computational domain. For incoming waves, however, they cannot be computed from outside the computational domain, and therefore additional physical considerations must be made. An important problem is how to identify the inward wave amplitude $L_i^{(x)}$. For an example, we will introduce the method of calculating $L_i^{(x)}$ for subsonic outflow and inflow in x-direction.

Subsonic outflow, inward wave amplitudes are addressed as:

$$L_1^{(x)} = \alpha(p - p_\infty) + (1-a)\Im_1^{(x)} + V_1^{(x)} \qquad x = l_x \tag{5}$$

$$L_5^{(x)} = \alpha(p - p_\infty) + (1-a)\Im_5^{(x)} + V_5^{(x)} \qquad x = 0 \tag{6}$$

Here, $\Im_i^{(x)}$ and $V_i^{(x)}$ denote the transverse and viscous terms, respectively. α and a are the relaxation coefficient of the pressure and transverse term, respectively.

The former standard NSCBC [1] is given by:

$$L_i^{(x)} = \alpha(p - p_\infty) \tag{7}$$

The equation (7) considers the effect of pressure relaxation only, and neglect the effect of the transverse and viscous terms. When these terms effect weakly in some flow condition, it will not influence the resolution and stability of numerical simulation. When the derivative of physical quantity in transverse terms is large enough for some flow simulations, this approximation can cause numerical instability and numerical reflection. We will explain it in details in the following part, and prove the scientism and rationality of Navier-Stokes characteristic boundary conditions with transverse and viscous effects.

Similar to pressure relaxation method, improved subsonic inflow boundary conditions [11] are adopted in this paper. In the treatment of the nonreflecting inflow, the inlet values of the flow velocity vector and temperature are imposed by using a set of relaxation terms. The modified LODI relations correspond to a set of linear relaxation constraints between the inflow variables and their prescribed

upstream values. Comparing with direct subsonic inflow conditions [1], this method has wider applicability, and superiority. In x-direction, subsonic inflow, inward wave amplitudes are addressed as:

$x = 0$:

$$L_2^{(x)} = \beta_2(T - T_0) + \Im_2^{(x)} + V_2^{(x)} \qquad L_3^{(x)} = \beta_3(v - v_0) + \Im_3^{(x)} + V_3^{(x)}$$

$$L_4^{(x)} = \beta_4(w - w_0) + \Im_4^{(x)} + V_4^{(x)} \qquad L_5^{(x)} = \beta_5(u - u_0) + \Im_5^{(x)} + V_5^{(x)} \qquad (8)$$

$x = l_x$:

$$L_1^{(x)} = \beta_1(u - u_{l_x}) + \Im_1^{(x)} + V_1^{(x)} \qquad L_2^{(x)} = \beta_2(T - T_{l_x}) + \Im_2^{(x)} + V_2^{(x)}$$

$$L_3^{(x)} = \beta_3(v - v_{l_x}) + \Im_3^{(x)} + V_3^{(x)} \qquad L_4^{(x)} = \beta_4(w - w_{l_x}) + \Im_4^{(x)} + V_4^{(x)} \qquad (9)$$

where T_0, u_0, v_0, w_0 and $T_{l_x}, u_{l_x}, v_{l_x}, w_{l_x}$ is the accurate value of physical variables at the inflow boundary, β_i is the corresponding relaxation coefficients.

It has paid many attentions that control quantities of Navier-Stokes equations in the conservation form are conservation variables, but the physical boundary conditions are usually expressed by primitive variables and their derivatives. In this paper, equations (1) are directly solved using primitive variables expressed by Sutherland's method [10]. For the corner point, the characteristic method is applied simultaneously in both directions, and the boundary condition is given by:

$$\frac{\partial}{\partial t}\begin{bmatrix} u \\ v \\ w \\ \rho \\ p \end{bmatrix} + \begin{bmatrix} (L_5^{(x)} - L_1^{(x)})/\rho c \\ L_3^{(x)} \\ L_4^{(x)} \\ L_2^{(x)} + (L_5^{(x)} + L_1^{(x)})/c^2 \\ L_5^{(x)} + L_1^{(x)} \end{bmatrix} + \begin{bmatrix} M_2^{y} \\ (M_5^{(y)} - M_1^{(y)})/\rho c \\ M_4 \\ M_3^{(y)} + (M_5^{(y)} + M_1^{(y)})/c^2 \\ M_5^{(y)} + M_1^{(y)} \end{bmatrix} + \begin{bmatrix} T_1 \\ T_2 \\ T_3 \\ T_4 \\ T_5 \end{bmatrix} = \begin{bmatrix} d_u \\ d_v \\ d_w \\ d_\rho \\ d_p \end{bmatrix} \qquad (10)$$

$$M^{(y)} = (M_1^{(y)}, M_2^{(y)}, M_3^{(y)}, M_4^{(y)}, M_5^{(y)})^T$$
$$= [\lambda_1^{(y)} \cdot \frac{1}{2}(\frac{\partial p}{\partial y} - \rho c \frac{\partial v}{\partial y}), \lambda_2^{(y)} \frac{\partial u}{\partial y}, \lambda_3^{(y)}(\frac{\partial \rho}{\partial y} - \frac{1}{c^2}\frac{\partial p}{\partial y}), \lambda_4^{(y)} \frac{\partial w}{\partial y}, \lambda_5^{(y)} \cdot \frac{1}{2}(\frac{\partial p}{\partial y} + \rho c \frac{\partial v}{\partial y})]^T$$

$$T = [w\frac{\partial u}{\partial z}, w\frac{\partial v}{\partial z}, w\frac{\partial w}{\partial z} + \frac{1}{\rho}\frac{\partial p}{\partial z}, \frac{\partial(\rho w)}{\partial z}, w\frac{\partial p}{\partial z} + \gamma p\frac{\partial w}{\partial z}]^{\mathrm{T}} \qquad (11)$$

where $\lambda_k^{(y)}$ are the characteristic velocities

$$\lambda_1^{(y)} = v - c, \lambda_2^{(y)} = \lambda_3^{(y)} = \lambda_4^{(y)} = v, \lambda_5^{(y)} = v + c \qquad (12)$$

3. NUMERICAL TEST AND ANALYSIS

In the numerical simulation of Navier-Stokes equations, six order compact schemes are adopted for transverse terms and viscous terms, and three order and four order compact schemes are applied in the boundary points and near boundary points, respectively. Four step Runge-Kutta method is used in the time-integartion. The artificial dissipation [14] is replaced by eight order filters. Next, numerical test of some typical flows is studied and analyzed.

3.1 Vortex convection in the free flow

The two-dimensional vortex convects through a non-reflecting boundary. This is a typical test used to evaluate boundary conditions. The configuration corresponds to a single vortex in a uniform flow field along the x_1-direction. The initial flow field is prescribed by:

$$\begin{pmatrix} u \\ v \end{pmatrix} = \begin{pmatrix} u_\infty \\ 0 \end{pmatrix} + 1/\rho \begin{pmatrix} \dfrac{\partial \Psi}{\partial y} \\ -\dfrac{\partial \Psi}{\partial x} \end{pmatrix}, \qquad \Psi = C \exp\left(-\frac{(x-x_0)^2 + (y-y_0)^2}{2R_c^2}\right) \tag{13}$$

where Ψ is a stream function for an incompressible vortex, C is the vortex strength , R_c is the vortex radius , and (x_0, y_0) is the location of the vortex center[1]。 The initial pressure field corresponding to the vortex is given by:

$$p = p_\infty - \rho \frac{C^2}{R_c^2} \exp\left(-\frac{(x-x_0)^2 + (y-y_0)^2}{2R_c^2}\right) \tag{14}$$

The flow conditions are specified as $Ma = u_\infty / c = 0.1$ where Ma is Mach number, u_∞ is the free flow velocity, c is sound velocity, $R_c / l_x = 0.1$, $C/(cl_x) = -0.0025$. The domain size is $2.0mm \times 2.0mm$ with 200 grids in each direction. The reference temperature and pressure are 300K and 1 atm, respectively, and the fluid is air. The maximum velocity induced by the vortex is $10.52cm/s$.

At the inflow boundary $x = 0$, standard non-reflecting subsonic inflow boundary condition [1] is applied. At the outflow boundary $x = l_x$, three different non-reflecting boundary conditions are tested by using A1, A2 and A3, respectively, in order to illustrate the effect of transverse term and viscous terms in boundary conditions.

A1: Standard non-reflecting boundary condition $L_1^{(x)} = \alpha(p - p_\infty)$ is adopted. From

equation (1), we can obtain the effective boundary condition:

$$(\frac{\partial p}{\partial t}-\rho c\frac{\partial u}{\partial t})=-2\alpha(p-p_\infty)+2(\Im_1^{(x)}+V_1^{(x)}) \tag{15}$$

A2: $L_1^{(x)}=\alpha(p-p_\infty)+\Im_1^{(x)}+V_1^{(x)}$ is applied, which is referred as Navier-Stokes characteristic boundary conditions with transverse terms and viscous terms. So the effective boundary condition has only pressure relaxation term in RHS:

$$(\frac{\partial p}{\partial t}-\rho c\frac{\partial u}{\partial t})=-2\alpha(p-p_\infty) \tag{16}$$

A3: The modified characteristic boundary condition (5) is adopted. The transverse term in $L_1^{(x)}$ has differences with the accurate vales of physical flows in some cases. Similar to the pressure relaxation method, relaxation of transverse term is adopted. In following standard asymptotic analysis at low Mach number flows [12], an estimate of an appropriate relaxation coefficient $a=Ma$ is derived, and effective boundary conditions become:

$$(\frac{\partial p}{\partial t}-\rho c\frac{\partial u}{\partial t})=-2\alpha(p-p_\infty)-2MaS_1^{(x)} \tag{17}$$

In the y-direction, the standard non-reflecting boundary condition [1] is applied in test A1-A3.The additional viscous conditions are:

in y -direction: $\partial q_y/\partial y=0$, $\partial\tau_{yx}/\partial y=0$;

in x-direction: $\partial\tau_{xx}/\partial x=0$ $(x=0)$, $\partial q_x/\partial x=0$ and $\partial\tau_{xy}/\partial x=0$ $(x=l_x)$.

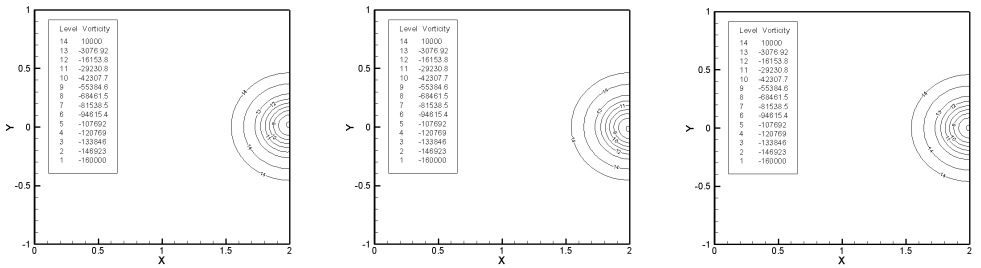

A1 **A2** **A3**

Fig.1 Vorticity isocontours $(1/s)$ at $t=28.8\mu$sec

The vorticity isocontours passing through the outflow boundary are shown in Fig.1 for A1-A3. No significant difference can be found, even if different boundary boundary conditions are used. The center region of the vortex for A1 and A2 are slightly distorted, showing an upward and downward motion at the

boundary, respectively. On the other hand, x, y velocity is shown in Fig.2. It reveals that the numerical artifacts arise because of the implementations of the incorrect boundary condition. From the isocontours, contrast to A3, A1 yields acceleration in the u velocity and a deceleration in the v velocity, while A2 leads to an opposite behavior.

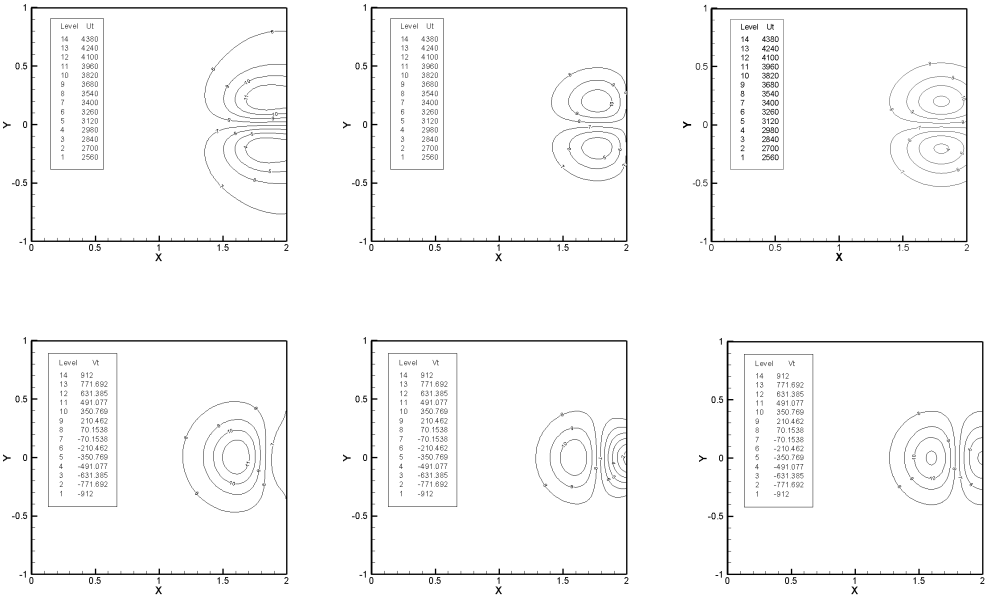

Fig.2 x, y velocity isocontours (cm/s) at $t = 28.8\mu$sec

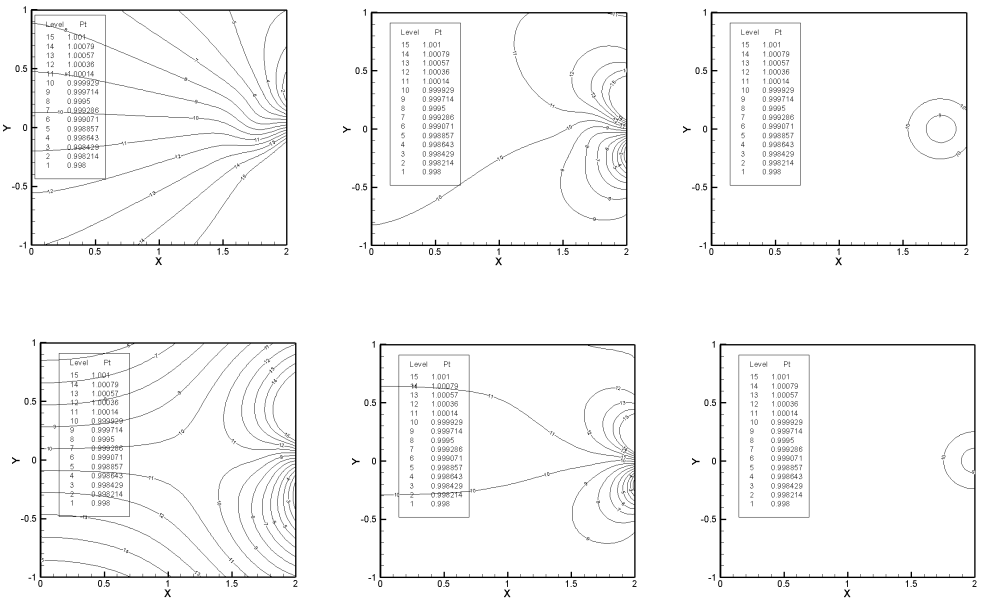

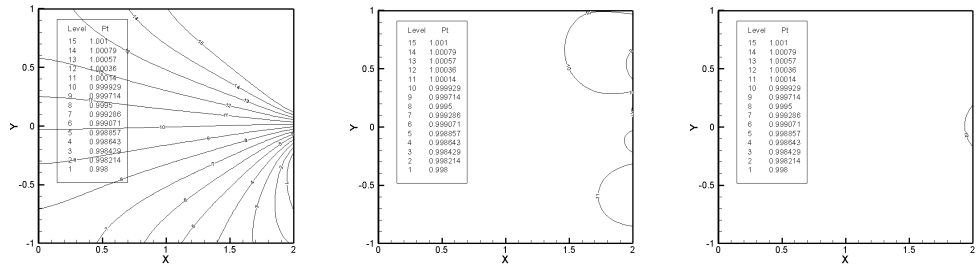

A1 **A2** **A3**

Fig.3 Temporal variations of pressure isocontours (atm).

(from top to bottom, t=23.0; 28.8; 34.56 μ sec)

The temporal variations of pressure isocontours for A1-A3 are shown in Fig.3. The results indicate that a significant amount of spurious pressure field generates at the boundary employing A1 condition without the transverse term and viscous term. The visible numerical reflecting appears from the velocity and pressure field, as the vortex travels out of the boundary and the shape changes. As the vortex approaches the boundary, the $\gamma p\dfrac{\partial v}{\partial y}$ term in equation (15) becomes dominant. Therefore, the effective boundary conditions cause the numerical reflecting, and these terms can not be ignored. The transverse term and viscous term are included in the boundary conditions for A2; hence the pressure variation is more confined near the boundary with smaller amplitude than those for A1. Since the leading order in equation (16) is $\rho c\dfrac{\partial u}{\partial t}=0$, its net effect is to damp out the x-direction velocity near the boundary. All the neglected terms are reconsidered for A3, and the transverse term relaxation is also adopted. The results show that there is not numerical reflecting in the pressure and velocity field, and the vortex shape does not change as it travels out of the boundary.

3.2 Counter flow

The counter flow is used in the boundary condition test. A true challenge occurs in a counterflow configuration where velocity needs to be imposed at the two opposing inflow boundaries. It is hard to control the inflow velocity and the absolute value of pressure. The modified inflow characteristic boundary condition is applied. Initial flow condition is same as C.S.YOO [11].Three different boundaries are tested and compared in this paper.

B1 : Modified inflow conditions (8) (9) are used in x-direction, but transverse term and viscous terms are not included. In the y-direction, standard characteristic boundary condition A1 is applied.

B2：Modified inflow conditions (8) (9) are used in x-direction, and transverse term and viscous term are considered. In the y-direction, standard characteristic boundary condition A1 is applied.

B3：Modified inflow conditions (8) (9) are used in x-direction, and transverse term and viscous term are considered. In the y-direction, modified characteristic boundary condition A2 is applied.

The results of B1 are shown in Fig.4, the u velocity isocounters is distorted, inlet velocity value changes, and the background pressure values can not maintain. The value in the center reaches 1.37 atm. The results of B2 are shown in Fig.5, the inlet velocity value is preserved, but the background pressure value become even large, reaches 1.49 atm in the center. Considering transverse terms in both directions, the results of B3 are shown in Fig.6. The inflow velocity and background pressure are both preserved. The center value of pressure is 1.0011 atm, which is as same as the reference's value [11]. Our numerical algorithms, which combines improved NSCBC method with high order non-dissipative compact schemes, has good reliability.

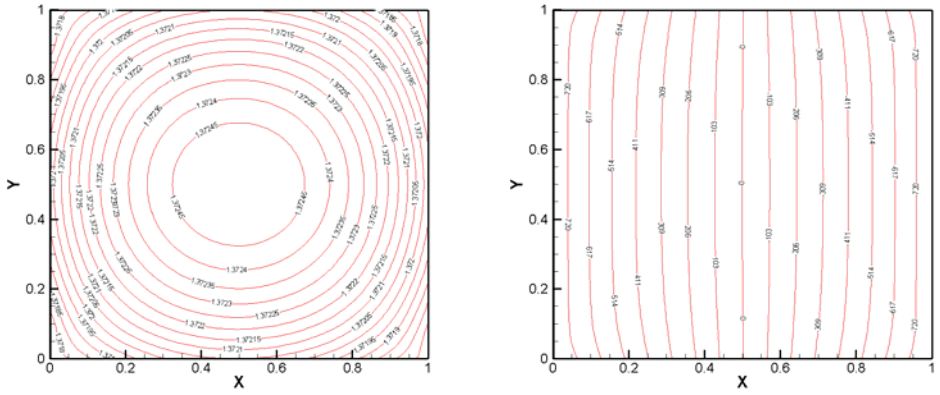

Fig.4 Pressure and x-direction velocity at $t = 10ms$ for condition B1

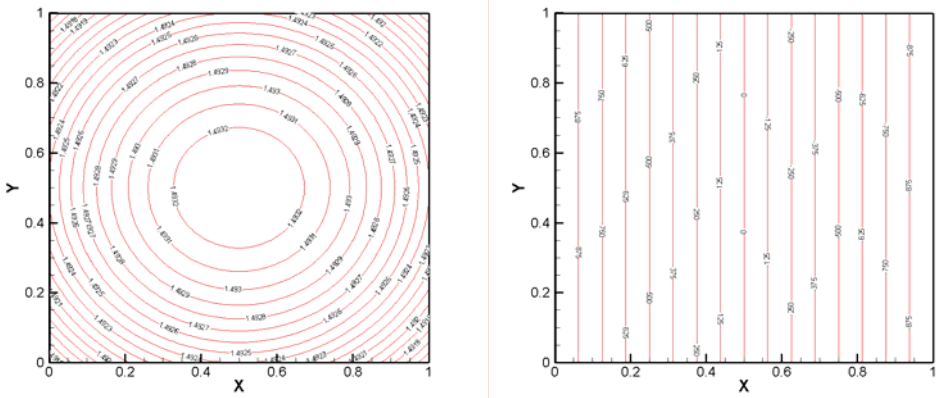

Fig.5 Pressure and x-direction velocity at $t = 10ms$ for condition B2

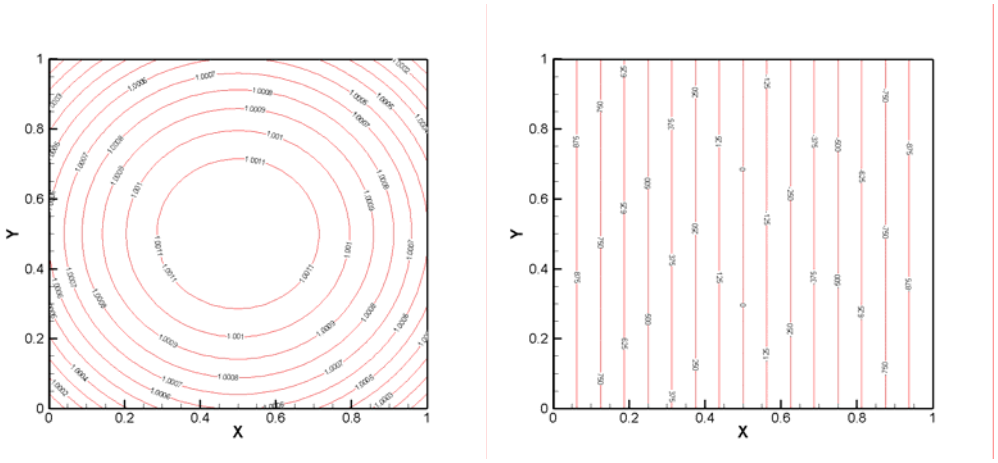

Fig.6 Pressure and x-direction velocity at $t = 10ms$ for condition B3

3.3 Pressure wave propagation in stationary flow

The pressure field is initialized with a pressure pulse:

$$\frac{\partial p}{\partial x} = A(x - x_0)e^{-B(x-x_0)^2+(y-y_0)^2}\sin(\omega t)$$
$$\frac{\partial p}{\partial y} = A(y - y_0)e^{-B(x-x_0)^2+(y-y_0)^2}\sin(\omega t) \qquad (18)$$

The reference variables for scale, density, velocity, temperature, pressure, time, viscosity are λ (wave length), ρ_∞, c, T_∞, $\rho_\infty c^2$, λ / c and μ_∞ respectively. The computational domain is a square ($xl \times yl = 12 \times 12$).The pressure wave is induced at center of the square. The parameters are $A = 0.005, B = 400, \omega = 2\pi$.Reynolds number is 10000.

Modified NSCBC is adopted at the boundaries. Pressure counters at time 2、4 and 6 are presented in Fig 7(a)、(b) and (c). As wave pass through the boundary, the pressure counter shows is displaied in Fig.7 (d). The distribution of pressure of x-direction centerline is shown in Fig.7(e) at time 20. Once the pressure front meets the boundary, the boundary condition is remarkably capable of preserving the correct physical information at the boundary edges and corners.

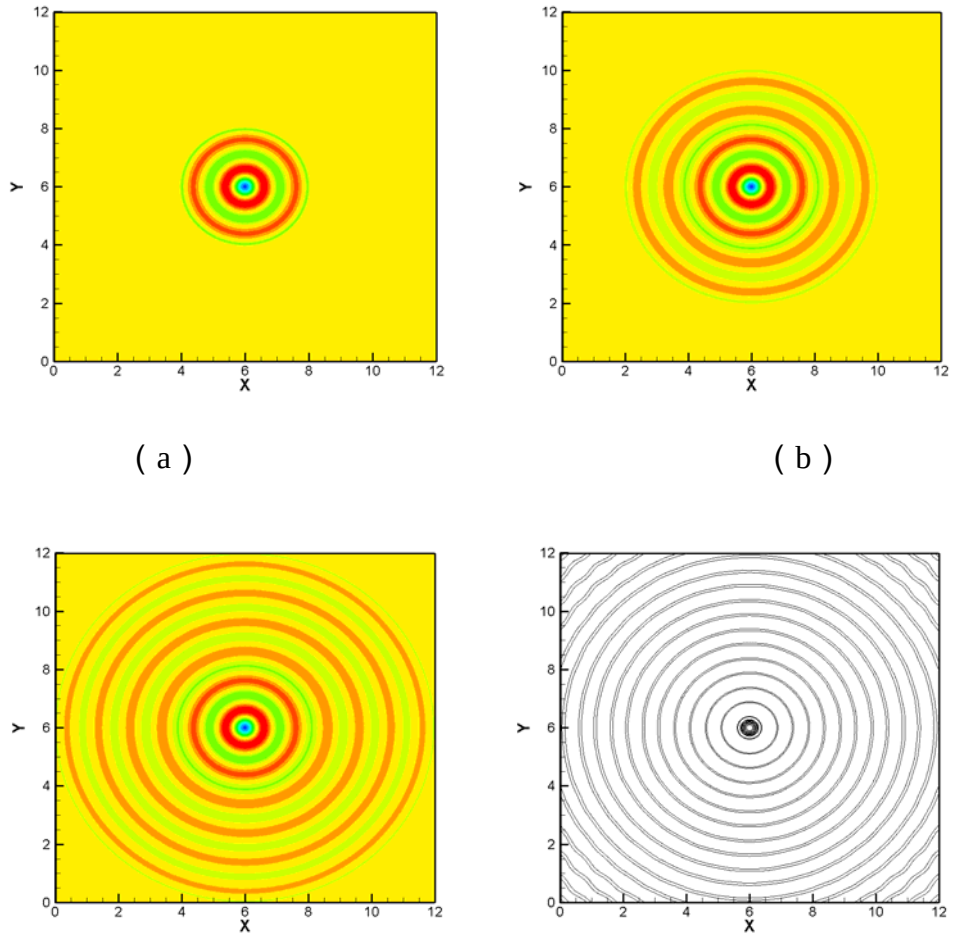

(a) (b)

(c) (d)

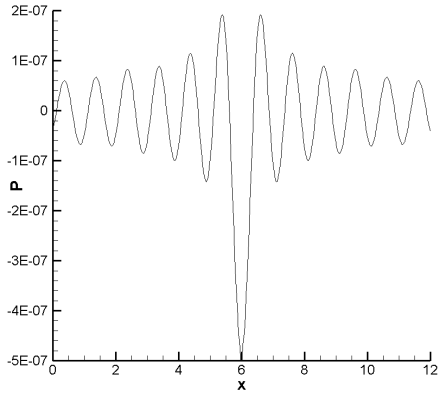

(e)

Fig.7 Evolution of the pressure distribution

3.4 Subsonic boundary layer flow over the flat plate

Next,we study the boundary layer flow over the flat plate at M_a=0.5 and Re=100 which is based on the inflow displacement thickness. The domain length and heights are both 30. The number of grid points is 64×32. The modified NSCBC condition is used at upper free stream flow and outflow boundary. The distribution of computational velocity and temperature normalized by the edge values at $x=55.7$ is shown in Fig.8. In spite of the quite low Reynolds number and coarse gird, comparing computational results with Blasius solution, the agreement is quite good. Fig.9 gives the pressure at the wall, which almost keeps the same, and there is nearly no non-physical pressure reflecting at the outflow boundary.

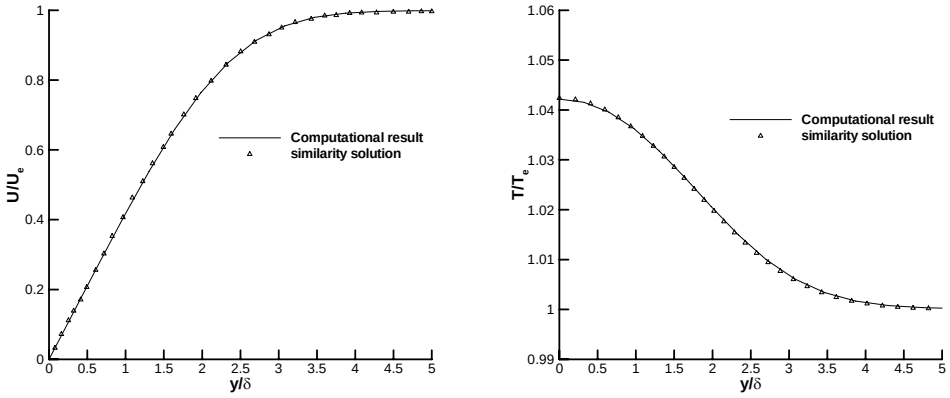

Fig.8 distribution of velocity and temperature at $x=55.7$

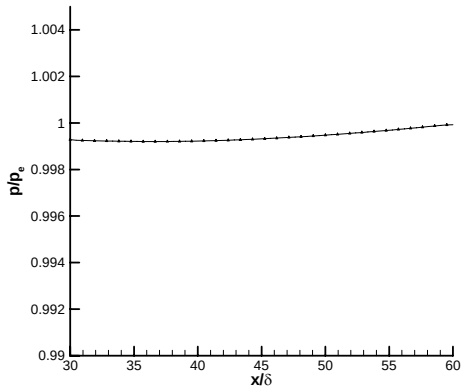

Fig.9 pressure at the wall

4 CONCLUSIONS

A number of lingering issues of spurious solution behavior has encountered in some flow simulations in the past using standard NSCBC. In these flows the

transverse terms and viscous terms affect the boundary conditions. Improved Navier-Stokes characteristic boundary conditions using high order schemes were adpoted in this paper. A couple of typical cases were tested to certificate the feasibility of the algorithm. This method has more convenient applicability, high resolution, and smaller reflecting wave amplitude at the boundary. Obviously, it is concluded that this algorithm is quite suitable for direct simulation of Navier-Stokes equations.

REFERENCES

[1] T.J.Poinsot and S.K.Lele, Boundary conditions for direct simulations of compressible viscous flow, Journal of Computational Physics, 101(1992), 104-139.

[2] K.W.Thompson,Time-dependent boundary conditions for hyperbolic systems, Journal of Computational Physics, 68(1987),1-24.

[3] K.W.Thompson,Time-dependent boundary conditions for hyperbolic systems, Journal of Computational Physics,89(1990),439-461.

[4] J.Oliger and A.Sundström, Theoretical and practical aspects of some initial boundary-value problems in fluid-dynamics, SIAM Journal on Applied Mathematics,35(1978):419-446.

[5] L.Halpern,Artificial boundary conditions for incompletely parabolic perturbations of hyperbolic systems, SIAM Journal on Mathematical Analysis,22(1991),1256-1283.

[6] P.Dutt,Stable boundary conditions and difference schemes for Navier-Stokes equations, SIAM Journal on Numerical Analysis, 25(1988),245-267.

[7] M.Baum, T.J.Poinsot and D.Thévenin, Accurate boundary conditions for multicomponent reactive flows, Journal of Computational Physics, 176(1994),247-261.

[8] N Okong'o and J Bellan,Consistent boundary conditions for multicomponent real gas mixtures based on characteristic waves, Journal of Computational Physics,176(1994),330-344.

[9] T.J.Poinsot and D.Veynante,Theoretical and Numerical Combustion, Second Edition. R.T.Edwards Inc, Philadelphia.2005.

[10] J.C.Sutherland and C.A.Kennedy,Improved boundary conditions for viscous reacting compressible flows, Journal of Computational Physics, 191(2003),502-524.

[11] C.S.Yoo,Y.Wang, A.Trouvé,and H.G. Im, Characteristic boundary conditions for direct numerical simulations of turbulent counterflow flames, Combustion Theory and Modelling, 9(2005),617-646.

[12] C.S.Yoo and H.G.Im, Characteristic boundary conditions for simulations of compressible reacting flows with multi-dimensional, viscous, and reaction effects, Combustion Theory and Modeling 11(2) (2007), 259-286.

[13] S.K.LeLe, Compact Finite Difference Schemes with Spectral-like Resolution, Journal of Computational Physics, 103(1991), 16-42.

[14] V.G.Datta and R.V.Miguel,High-order schemes for Navier-Stokes equations: algorithm and implementation into FDL3DI,AFRL-VA-WP-TR-1998-3060.

Received: August, 2009